

Fig. 2. Unified device encoding scheme based on finite element mesh details node and edge features with task-specific self-consistent quantities.

density as an additional feature, whereas the node features of the IV predictor included both charge density and potential. Architecturally, the Poisson emulator employed a deep graph attention network with edge feature (RelGAT) and comprised approximately 1 million parameters, incorporating a 12-layer GAT with 2 attention heads and one multilayer perceptron (MLP). In contrast, the IV predictor utilized a shallower RelGAT model with about 0.15 million parameters, featuring a 3-layer, single-head GAT with a 4-layer MLP for prediction. Layer normalization was applied in the training of both models, enhancing model convergence and stability across the dataset of 50,000 independent devices. Table II showcases the effectiveness of the RelGAT model, demonstrating its high accuracy through validation and testing. To further assess the generalizability, an additional test on 32,000 unseen data samples was conducted, indicating a highly accurate surrogate TCAD model.

TABLE II
MSE OF SURROGATE TCAD IN THE WHOLE TESTING DATASET

	Validation	Testing	Unseen(32K)	$R^2(32K)$
Poisson Emulator	6.17×10^{-5}	7.02×10^{-5}	7.15×10^{-5}	0.9999
IV Predictor	1.67×10^{-3}	1.60×10^{-3}	1.78×10^{-3}	0.9999

B. Unified Compact Model for Emerging Technologies

The compact model for emerging transistors is formulated to account for mobility variations in CNT, IGZO, and LTPS technologies due to charge drift in the presence of tail-distributed traps (TDTs) and variable range hopping (VRH) [3], as detailed in Eq. (1):

$$\mu = \begin{cases} \mu_0(V_G - V_{th})^\gamma, & \text{N-type TFT} \\ \mu_0(V_{th} - V_G)^\gamma, & \text{P-type TFT} \end{cases} \quad (1)$$

where V_{th} is the threshold voltage, γ is the field enhancement factor for mobility and μ_0 is defined as the effective mobility when $|V_G - V_{th}| = 1$. This model integrates mobility enhancement assumptions with the charge drift to develop an intrinsic current model. Validation against measured I-V curves from CNT, LTPS, and IGZO based devices is shown in Fig. 3.

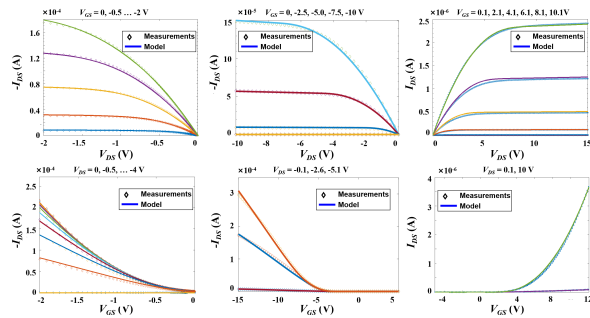


Fig. 3. Validations of the proposed TFT model with measured I-V curves: (a) CNT-TFT with $L = 25\mu\text{m}$ and $W = 125\mu\text{m}$; (b) LTPS-TFT with $L = 16\mu\text{m}$ and $W = 40\mu\text{m}$; (c) IGZO-TFT with $L = 20\mu\text{m}$ and $W = 30\mu\text{m}$.

C. GNN-based Fast Cell Library Characterization Model

Our methodology employs a two-stage process to advance cell characterization for semiconductor design. Initially, we developed a comprehensive cell library comprising 35 types

of combinational and sequential cells and utilized transistor-level SPICE simulation to generate extensive cell datasets for training and testing, encompassing nine metrics including delay, output slew, leakage power, capacitance (maximum capacitance of each input pin), flip power (dynamic power generated when both input and output pins are flipped), non-flip power (dynamic power generated when only the input pins are flipped, while the state of the output pin remains unchanged), minimum setup/hold time, and pulse width (for sequential cells only) under various corners and technology settings. In the second stage, we adopted a 3-layer graph convolutional network (GCN) to establish our framework. To enhance the accuracy of predictions, an additional 2-layer MLP was added after the GCN layers for each metric.

In our study of emerging technology, we utilized the unified compact model and specifically focused on analyzing the variation of supply voltage (V_{DD}), threshold voltage (V_{th}), and gate unit capacitance (C_{ox}). These three critical parameters significantly influences the performance of emerging devices. The definitions of node features are presented in Table III. Here, "Current_state" and "Next_state" are two features related to the input pin state, with "1" denoting a high level and "0" representing a low level, respectively. "Input_slew" denotes the transition time of input signal, "Output_load" denotes capacitive load on cell output pins. For cell metrics that do not have relationship with some bits in the vector, these bits will be set to "0".

TABLE III
NODE FEATURE VECTOR DEFINITION FOR SILICON TECHNOLOGY

	IN	OUT	N-FET	P-FET	V_{DD}	V_{SS}
Bit0	0	0	0	0	1	1
Bit1	0	1	1	1	0	0
Bit2	1	0	1	1	0	1
Bit3	0	0	-1	1	0	0
Bit4	0	0	0	0	V_{DD}	0
Bit5	0	0	Width	Width	0	0
Bit6	0	0	Gate Unit Capacitance	Gate Unit Capacitance	0	0
Bit7	0	0	V_{th}	V_{th}	0	0
Bit8	Input_slew	0	0	0	0	0
Bit9	0	Output_load	0	0	0	0
Bit10	Current_state	0	0	0	0	0
Bit11	Next_state	0	0	0	0	0

As detailed in Table IV, valid data from 125 corners were for training while from 512 corners for testing, the model demonstrated high accuracy in experiments. For flip power and non-flip power, the average error of prediction is relatively larger compared with other cell metrics, the reason is due to the fact that the dynamic power consumption varies by several orders of magnitude among different standard cells. The model exhibits a relatively large percentage error in predicting extremely low dynamic power consumption which needs to be improved in our future work.

TABLE IV
MAPES OF CELL LIBRARY PREDICTION IN THE WHOLE TESTING DATASET

	LTPS	CNT	Number of Data Points
Delay	0.47%	0.62%	696320
Output Slew	0.79%	0.83%	696320
Capacitance	0.18%	0.21%	70656
Flip Power	5.74%	4.96%	696320
Non-flip Power	3.36%	5.60%	393216
Leakage Power	2.78%	2.39%	165888
Minimum Pulse Width	1.20%	1.67%	8192
Minimum Setup	0.50%	0.27%	16384
Minimum Hold	0.45%	0.38%	16384

REFERENCES

- [1] E. M. Bazizi et al., "Materials to Systems Co-Optimization Platform for Rapid Technology Development Targeting Future Generation CMOS Nodes," in IEEE Transactions on Electron Devices, vol. 68, no. 11, pp. 5358-5363, Nov. 2021, doi: 10.1109/LED.2021.3076757.
- [2] W. Jang et al., "TCAD Device Simulation With Graph Neural Network," in IEEE Electron Device Letters, vol. 44, no. 8, pp. 1368-1371, Aug. 2023, doi: 10.1109/LED.2023.3290930.
- [3] L. Shao et al., "Compact Modeling of Thin-Film Transistors for Flexible Hybrid IoT Design," in IEEE Design & Test, vol. 36, no. 4, pp. 6-14, Aug. 2019, doi: 10.1109/MDAT.2019.2899058.
- [4] F. Klemme, Y. Chauhan, J. Henkel and H. Amrouch, "Cell Library Characterization using Machine Learning for Design Technology Co-Optimization," 2020 IEEE/ACM International Conference On Computer Aided Design (ICCAD), San Diego, CA, USA, 2020, pp. 1-9.
- [5] L. Xu, C. Qiu, L. Peng, and Z. Zhang, "Suppression of leakage current in carbon nanotube field-effect transistors," Nano Res., vol. 14, no. 4, pp. 976-981, Apr. 2021, doi: 10.1007/s12274-020-3135-8.